Master's Thesis
석사 학위논문

Fabrication of Magnetically Rotating Active Micromixer and Evaluation of Mixing Performance

Jinhyuk Kim (김 진 혁 金 眞 赫)

Department of Robotics Engineering
로봇공학전공

DGIST

2014

Master's Thesis
석사 학위논문

Fabrication of Magnetically Rotating Active Micromixer and Evaluation of Mixing Performance

Jinhyuk Kim (김 진 혁 金 眞 赫)

Department of Robotics Engineering
로봇공학전공

DGIST

2014

Fabrication of Magnetically Rotating Active Micromixer and Evaluation of Mixing Performance

Advisor : Professor Hongsoo Choi

Co-advisor : Professor Yongsoon Eun

By

Jinhyuk Kim
Department of Robotics Engineering
DGIST

A thesis submitted to the faculty of DGIST in partial fulfillment of the requirements for the degree of Master of Science in the Department of Robotics Engineering. The study was conducted in accordance with Code of Research Ethics[1]

01. 10. 2014

Approved by

Professor Hongsoo Choi (Signature)
(Advisor)

Professor Yongsoon Eun (Signature)
(Co-Advisor)

[1] Declaration of Ethical Conduct in Research**:** I, as a graduate student of DGIST, hereby declare that I have not committed any acts that may damage the credibility of my research. These include, but are not limited to: falsification, thesis written by someone else, distortion of research findings or plagiarism. I affirm that my thesis contains honest conclusions based on my own careful research under the guidance of my thesis advisor.

Fabrication of Magnetically Rotating Active Micromixer and Evaluation of Mixing Performance

Jinhyuk Kim

Accepted in partial fulfillment of the requirements for the degree of Master of Science.

12. 03. 2013

Head of Committee	최 홍 수	(인)
	Prof. Hongsoo Choi	
Committee Member	은 용 순	(인)
	Prof. Yongsoon Eun	
Committee Member	장 재 은	(인)
	Prof. Jae Eun Jang	

MS/RT
201223003

김 진 혁. Jinhyuk Kim. Fabrication of Magnetically Rotating Active Micromixer and Evaluation of Mixing Performance. Department of Robotics Engineering. 2013. 46p. Advisor Prof. Choi, Hongsoo, Co-Advisor Prof. Eun, Yongsoon.

ABSTRACT

The micro mixers are essential to mix the fluids in lab-on-a-chips which analyze the biological antigen-antibody reactions or chemical reactions. The fluids flowing in lab-on-a-chips have very low Reynolds number which is under 100. Fluids having a low Reynolds number are mainly depend on diffusion mechanism to mix when flowing in a micro channel. Therefore, the mixers using the diffusion mechanism need very long channel length and narrow channel width for efficient mixing. However, these kind of passive mixers using the diffusion mechanism have limitations in their sample size caused by the long channel length. Thus, researchers have studied to overcome the limitations of passive mixer to achieve good mixing performance in limited device size. One way to achieve this goal is generating chaotic advection in the microfluidic system.

In this thesis, fabrication of magnetically rotating active micromixer was studied and the mixing performance was evaluated. The rotating motion is efficient to increase the contract area between the fluids and the rotor which is spun by external rotating magnetic field. The rotating magnetic field initiates the

rotational movement of the rotor by generating magnetic torque. The rotor was fabricated by electroplating using a magnetic material which is Nickel-Cobalt alloy to enhance the magnetic torque. In addition, the micro fluidic channel was designed in simple Y-shape with two inlets and one outlet to evaluate the mixing performance. The different color dyed fluids are injected at each inlet and the fluids are mixed at the mixing chamber.

The experimental setup except the micromixer consists of the three parts; syringe pumps, a high speed camera, and a rotating magnet connected with a DC motor. The motor generates the rotational field and the rotational speed can be controlled by changing RPM of the motor. The syringe pumps were used to inject and extract the fluids to the inlets and from the outlet, respectively. The mixing performance of the micromixer was evaluated by captured images using the high speed camera. The mixed fluids were analyzed to obtain the intensity of each pixel by converting the image into gray scale. The mixing performances are expressed by using standard deviation and normalized pixel intensity.

The mixing performance was evaluated with various conditions. The flow rate was varied from 10 μL/hr to 500 μL/hr, and the used voltages of the motor were 6 V and 8 V. Reynolds numbers were calculated for each flow rate that are 0.064 and 0.0013 for 500 μL/hr and 10 μL/hr, respectively. If the standard deviation of color index with gray scale is zero, the mixing performance is defined to be 100%. The highest

mixing performance was 90 percent with Reynolds number of 0.01.

Different mixing performances along with the different rotor shapes were investigated with a constant voltage, 6V, into the motor. The mixing performances of the Z-shaped rotor and I-shaped were varied from 90 to 77 percent and 83 to 65 percent for 100 μL/hr and 500 μL/hr, respectively. Thus, the Z-shaped rotor showed better performance around 10% than the I-shaped rotor.

However, when applying 8 V into the motor, the mixing performances were not much difference with the two different rotor shapes. For the Z-shaped rotor, the mixing performance was nearly saturated at 6 V so, when applying 8 V into motor, the mixing performance was barely changed. On the contrary, the I-shaped rotor was not reached at the saturated status at 6 V. Thus, the mixing performance of the I-shaped rotor was increased until 8 V and saturated at this condition. For this reason, when comparing the mixing performance of the Z-shaped and I-shaped rotors, the difference of each rotor was small when applying 8 V into the motor.

Keywords: Magnetic rotor, Micromixer, Magnetic actuation, Microfluidic channel, Image analysis

Contents

List of Tables

List of Figures

1. INTRODUCTION

1.1 Background

Studies about Micro Electro Mechanical Systems (MEMS) technology started from the late 1980s and have been increasing until now [1]. MEMS technology was derived from semiconductor process technology to miniaturize conventional sensors, actuators, and transducers. Mass produced MEMS devices can be integrated with signal processing unit such as Complementary metal-oxide semiconductor (CMOS) or Application specific integrated circuit (ASIC) and they can be operated at low power [2]. Furthermore, MEMS community has been trying to make valuable products or improve the fabrication process by combining MEMS devices with other disciplines such as Biotechnology (BT). The Lap-on-a-chip (Lab chip) and Micro Total Analysis System (μ-TAS) are typical examples of the applications of MEMS for BT [3].

Biochips made from glass, silicon, or plastic materials allow analysis of the reaction of gene expression, congenital defects, and protein distribution using the cell, antibody-antigen reaction. These biochips will be changing the field of medicine development, clinical diagnosis, and science technology research parts and it will be rapidly supplying to us. Biochips which can diagnose cancer and Acquired Immune Deficiency Syndrome (AIDS) have been developed [4]. In addition, the biochips application will be used in agriculture, the food industry, and environment monitor, it will also be furnished.

The biochips are divided into two categories: micro array chip and micro fluidic chip. Micro array chips are a collection array which consist of thousands of Deoxyribonucleic acid (DNA) spots or protein spots

attached to regular internal on surface[5]. The chips quantify the expression levels of a great number of genes at the same time or to genotype multiple parts of a genome. On the other hand, micro fluidic chips are called Lab chip. The μ-TAS and the Lab chip are micro biochips that combine one or several laboratory tasks on a chip[6]. These devices contain all the steps needed for chemical and biological analysis of a sample on a single chip that is only a few square centimeters or millimeters in size. In addition, when using the micro biochip, it can carry out preprocess, separation, detection and observation of the reaction of the samples [3]. It can help workers or researchers by setting the automatic system using chip arrays. It observes the reaction of all process in biological material with high efficiency and speed. These devices can be goods which are very high value product [7-9]. Popular examples of these devices are the cell separation system, hemocytometer and biosensor [10, 11].

As aforementioned, there are several advantages when the micro scale fluidic channels use to analyze the biological experiment and other field. The size of the internal reaction space of microchips decreases to the micro scale experiment, the surface area-to-volume ratio is increased [12], and it means that the contact area is increased at the same flow rate. The downsizing brings the efficiency enhancement of chemical reaction and antibody-antigen reaction during a short time. Thus, it saves the cost, sample, time, and reagent because it only uses a few hundreds milliliters to Pico liters when analyzing the test samples. In addition, the downsizing helps the uniform reaction due to increasing the heat and mass transfer by the high surface area-to-volume ratio [1, 13]

1.2 Necessity of micromixer

The Lab chip consists of four parts mechanically; the pumps, the valves, the channel, and the mixer. The pumps make flow. The stream is controlled by the valves. The fluids is able to flow in the channel. Finally, the fluidics are mixed by the mixer. The mixing process is necessary to observe the reactions between the samples and reagent uniformly in Lab chips and μ-TAS. However, there are challenges to design the mixer and channel because the chips have a low Reynolds number. To design the chips, we need to understand the features of micro systems.

The characteristic of fluid flowing in the micro channel was explained by a Reynolds number. The Reynolds number was by comparing inertial force with viscosity force [14] by

$$\mathrm{Re} = \rho \cdot V \cdot L / \mu = \ inertial\ force / viscosity\ forces \qquad \textbf{(1.1)}$$

where μ is the dynamic viscosity of the fluid, L is the length or hydraulic diameter of the pipe, V is the mean velocity of the fluid, and ρ is the density of the fluid. Reynolds number explains the state of fluid whether it is s laminar flow or turbulent flow.

Assuming fully developed flow, when Reynolds number is below 2300, the flow is called laminar flow, and when Reynolds number is above 4000, the flow is called turbulent [15]. The macro scale fluids with high a Reynolds number and the micro scale fluids with low a Reynolds number have a few differences. One of the differences is that the momentum has large portion to transfer the mass in the macro scale, whereas the diffusion dominates to move the mass relatively in the micro region. In other words, when having low Reynolds number,

it means that the rate of viscosity is larger than the inertia about the Reynolds number. The chips, which are designed by micro fluidic channel, have a Reynolds number under 100. The flow of fluidic influences the viscosity dominantly.

A micromixer system is different mixing mechanism of macro scale. The reason is that the turbulence is made hardly in micromixer system which has the low characteristic length and flow rate. That why we cannot expect the mixture by turbulence. The most of mixture occurs by the diffusion of fluidics in micro scale. The diffusion can mix the fluid, but the performance is not enough to mix the all thing. When channel length is fully long, the fluidics can be mixed perfectly. However, there are limitations because the size of chips is fixed and the fabrication process is hard to realize all structure such as complex 3-dimansional structure. Thus, we cannot design the chip which has channel with long length which is enough to mix completely. In addition, it takes a long time to mix because the flow rate is very slow. The Equation (1.2) [16] shows the necessary time to mix in channel by

$$V = A\sqrt{Dt} \qquad \textbf{(1.2)}$$

A is the contact area between the liquid solutions being mixed and *D* is the diffusion constant. The time for mixing is reduced by increasing the area *A* with a given fluid volume. To make strong disturbance with effect, the following principles is studied energetically. The principles which are chaotic advection mechanism, fluid division and combination, channel extend, channel fold and fluidic dispersion help to improve the mixing performance efficiently. It means when increasing the contact area increases or closing the diffusion distance or

leading the intense disturbance to flow, the mixing performance is enhanced. To mix the fluids effectively, we need to study about the micro fluidic and mix.

1.3 Trend of related research

The micromixer is generally divided into passive mixer and active mixer [17]. Passive mixers have micro pillars which are located in micro channel and micro chamber to mix the fluidics. In some case, it has a complex three-dimensional structure in channel. The advantage of passive type is easily able to integration with micro devices and chips, and manufacture. Above all, it does not need the external energy so it structure is simple. Therefore, research in order to integrate microchips and μ-TAS is studied. However, it cannot show the stronger performance compared to the active mixers. Thus, it is necessary to arrange the fine structure in channel for thorough mixture or has narrow channel being enough to short width for diffusion. However, when having the narrow channel or many fine structures in channel, it causes pressure drop or channel length become longer.

On the other hand, the active mixer has the advantage of good mixing performance relatively by using a mixer using a strong interference caused by additional external energy. However, it needs the additional process for external energy, it has an actuator for moving in channel so it is hard to manufacture and assemble other parts. Furthermore, it is hard to use biological and micro chemical filed due to having the strong electrical field or strong magnetic field.

1.3.1 Passive type micromixer

The passive mixers are researched with multi-layer structure and chaotic advection mechanism. The multi-layer mixers separate the channels to increase the contact area and reduce the diffusion length between the fluid being mixed. After this, it combines the channels separated. The chaotic advection mixers generate the verticality direction velocity field against the flow velocity field. The powerful disturbance generated by the verticality direction velocity field enhances the mixing performance.

Bessoth designed the micromixer which has 16 channels to separate fluidic, and combine the separated channel after mixing. Not only was the mixing process visualized by the fluorescence dyeing method and microscope, but also mixing performance was evaluated. The time for 95 percent mixing performance requests the 40 millisecond. When mixing the fluid perfectly, the time needs the 100 millisecond [18].

Hessel suggested the 15 channels which have 60 μm widths, and it crossly disembogues fluid into channel. This concept is the reduction of diffusion length by flowing the split fluid, and causes inducing the uniform mixture. It also evaluated the mixing performance using the color dying method and the rhodanide method. The color dyeing method is digitized the intensity difference of two fluid which are the color dyed fluid and another one is non-dye fluid. The rhodanide method uses the chemical reaction between iron ion and rhodanide solution [19].

Schwesinger [20] and Branebjerg [21] used the 3-dimensional channels to mix. Two flows run the horizontality channel and the vertical channel, two channels were crossly arranged and are separated and combined to make uniform. However, the stream was crushed because the sudden change of a channel shape.

Thus, they could not show the planed result. After that, to reform the stream, Schonfeld fabricated the Split and recombine (SAR) micromixer [22].

Strook placed the askew furrows at the bottom of channel; the oblique grooves generate the 3-dimensional helical form flow. Based on the 3 dimensional helical form flows, the Strook designed the mixer which has the herringbone structure at the outside bottom of channel. The herringbone structure generated the intersect velocity field. The intersect velocity field got the chaotic advection which changes the position of parabolic point periodically [3].

1.3.2 Active type micromixer

The active type mixers were also researched to mix using various methods. Glasgow mixed two fluidic generating the disturbance changing the flow periodically. The change of cyclical flow was identified by analysis on numerical value causing the expansion and fold of flow. In addition, it showed the result experimentally when controlling the change of flow recurrently [23]. Niu modified enhancing the mixing performance by combining the cyclic changing flows into one flow and showed the better result than previous experiment due to improving the expansion and fold [24]. Oddy's mixer changed the electrical field around flow to make the expansion and fold [25]. Bau's mixer also changed the magnetic field to make the disturbance. Two case have the good mixing performance and mix flows uniformly [26].

1.4 Objective of research

Micromixer is one of the components of the Lab chips and μ-TAS, and device to blend the micro flow efficiently. This paper consists of the design the micromixer, fabrication, and evaluation of mixing performance. Micromixers need the uniformly mixing performance, low pressure drop, rapid mixture and easy integration. The conditions are necessary to analysis the sample speedily and accurately.

This paper researched the active mixer to make better performance than passive mixer. To make the active mixer, we used the rotating magnetic field which is generated by rotating magnet bar. The magnetic bar was attached on spin plane which is connected with motor. The rotating magnetic field spins the rotor made by Nickel-Cobalt alloy. Designed mixer can rotate without the center hub to fix the rotor. The non-hub mixer can assemble rotor and micro channel easily, and save the cost. In addition, it can control motor rotating speed and sense of rotation. The mixing performance was evaluated by using color dyeing method.

2. DESIGN AND FABRICATION

2.1 Design

The micromixers have to get a good performance and the high capacity to exactly analysis the samples for short time. The micro biochips handle with biology and chemical so, bear the acidic environment and the biocompatible commonly. In addition, a power to move the mixers have to be chosen minor damage source against samples because the samples are sensitive about the thermal effect and electrically. The pressure drop in channel is hot issue. When generating the pressure drop in micro channel, the inlet pumps need the high injection energy. However, when applying the high injection energy, the bonded area may lose the adhesive. The micromixers are able to integrate the other part such the reactors, and the heat exchangers. Finally, the micromixers can be fabricated by spending low cost, mass production, and easily assembling.

2.1.1 Micro rotors

In order to enhance the mixing performance, previous works have been dedicated to expand the contact area between two fluids [27]. We also chosen the rotate type mixer to expand the contact area between two fluids, and the power source to rotate the mixer is chosen the magnetic field. In addition, to generate the chaotic advection in micro scale mixing chamber, there are many actuation mechanism such electro field, ultrasound, and thermal. However, among the many actuation mechanism, magnetic actuation has convinced benefit above other methods because of their mighty forces to act on large displacements and innocuous to cells for the biochip application [28].

To rotate mixer following the spin magnetic field, we chosen the Nickel-Cobalt alloy material for micro mixer. The Nickel-cobalt alloy is ferromagnetic material and can be made by electroplating. When using the electroplating process, the shape of rotor can be made complexly 2-dimensionally by using photolithography process.

The material of rotor has to be suitable for rotation and light because of the friction between the rotor and substrate. In addition, the contact area has to be extensive to mix, and the symmetry form of stir-bar shape is suitable to spin without eccentricity.

The parameter of rotors are in the following. The Z-shaped rotor has a 20-μm-height and a 1150-μm-diameter. The I-shaped rotor has a 20-μm-height, a 950−μm-length, a 300-μm-width. The width of I-shaped rotor is possibility to sticking at 250-μm channel. Thus, to prevent from stuck in channel, the width is higher than channel width.

2.1.2 Micro fluidic channel

The channel width and height are important variable of mixing performance. When the channel width and height is sub-scores micrometer, the diffusion length is very short so the diffusion occurs easily. However, we want to know the mixing performance of mixer objectively. Thus, we decided the channel width to 250 μm and the height to 60 μm. In addition, the designed mixer chip has two inlets and one outlet. The two inlets inject the two different color ink to observe the mixing process. The shape of channel is Y-shape, and the cross-section of channel is rectangle because the photolithography process is used to fabrication.

The channel structure is made by Poly dimethyl-siloxane (PDMS). The reason chosen the PDMS is transparency of material. It means the chemical reactions and mixing process can be observed. In addition, the mixing performance is commonly evaluated by using dye fluidic or pH indicator. Therefore, PDMS is suitable for the micro channel.

2.2 Fabrication Process

2.2.1 Fabrication process for micro rotors

The fabrication flow chart for the micro rotor used an electroplating process. The fabrication process is explained in figure. The fabrication of the micro rotor started with a 300 nm wet thermal oxidation process (Figure 2.1 (a)). After the wet thermal oxidation process, 30 nm of titanium (Ti) was sputtered onto the oxidized wafer to serve as an adhesive and another 150 nm thick layer of copper (Cu) was sputtered to provide a seed layer for electroplating growth of the Nickel-Cobalt alloy (Ni-Co alloy) which is a ferromagnetic material (Figure 2.1 (b)). After, 30 μm thick photoresist (JSR TBH 151N) is spin-coated, and exposed to make mold for micro rotor (Figure 2.1 (c), (d)). Figure 2.1 (c) and (d) contain the information to make mold for electroplating. The mold is made in three steps. First step is spin-coat to wafer; the thickness of photoresist was controlled by RPM of wafer. The wafer rotates at 300 RPM during the 25 sec to first spread-out and take a break for 25 sec. After that, second spread-out is taken by 300 RPM during 10 sec, and finial main spin is conducted by 2000 RPM for 30 sec. Second step is soft bake at 110 ℃ for 5 min. third step is exposure at UV to develop the pattern.

The exposure energy is 500 mJ /cm2. Final step is developing which soak the coated wafer in developer solution (THB-DVL-1000) for 7min to get the rotor mold. Figure 2.1 (e) shows the making of the rotor using the electroplating process. The height of made rotor is 30 μm before the Chemical mechanical Polishing (CMP). After the CMP process, the rotor height is 20 μm (Figure 2.1 (f)). Finally, the rotor is completed by removing the adhesion, seed layer, and photoresist layer (Figure 2.1 (g), (h)). The photoresist was removed by THB-STR-1000 (JSR) solution at 80 ℃, and the cupper etchant and titanium etchant are removal the seed layer and adhesion.

Figure 2.3 (a) and (b) are the fabricated rotors. The Z-shaped rotors have 20 μm-height and 1150 μm-length (Figure 2.3(a)). The tolerance between rotor and mixing chamber is 40μm when assembling the channel with rotor (Figure 2.4 (a)). The I-shaped rotors have 20μm-height and 960 μm-length When assembling the channel with rotor (Figure 2.3(b)). The tolerance between rotor and mixing chamber is 135μm when assembling the channel and rotor (Figure 2.4 (b)).

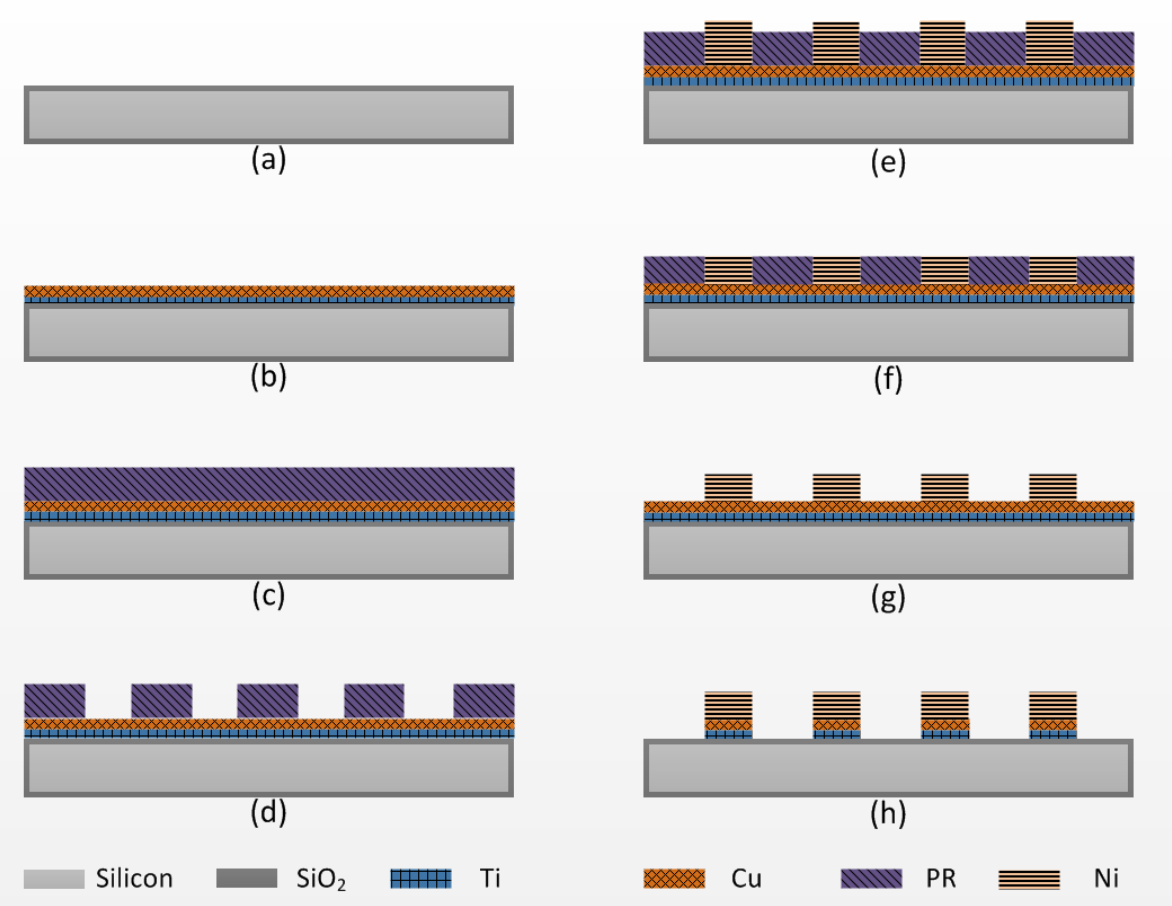

Figure 2.1 The flow chart to fabricate Nickel Cobalt alloy micro rotor: (a) the oxidation on bear wafer, (b) the sputtering the cupper and titanium for seed layer and adhesion layer, (c), (d) the spin-coating process and the exposure process making the electroplating mold, (e) the electroplating process to make the rotors, (f) the CMP process, and (g, h) the strip process.

2.2.2 Fabrication process for micro fluidic channel

Commonly, a Reactive Ion Etching technique (RIE) is used to fabricate the micro fluidic channel on silicon wafers. The channel, which is formed by silicon manufacturing technology, is utilized directly in micro fluidic devices. When using the RIE process, it requires very expensive facilities. There are challenges to implementing the high aspect to ratio, alternative techniques have to cost less than the popular fabrication

process [29]. To fabricate microfluidic channel in this thesis, different material and fabrication process were used.

The micro molding technique is one of the MEMS technologies. This technique uses the plastic material and polymer to build the structure. In addition, it can be mass produced with low cost. Thus, we decided master mold technique to make a channel.

To fabricate the micro fluidic channel mater mold, SU-8 2075 (Micro CHEM) is used for mold photoresist which is negative tone photoresist. Designed configuration of micro fluidic channel has been fabricated the photoresist layer on a silicon substrate (Figure 2.2 (a)). The height of the photoresist is 60 μm, in other words, it is height of the channel. The pattern of the channel was developed by a mask that consists of a Film Combine Glass (FCG) (Figure 2.2 (b)). The spin-coating and patterning process were made by six steps; spin-coating, soft bake, exposure, post-bake, development, and hard bake. The spin-coating process consists of spread-out spin and main spin. First spread-out process operates on 500 RPM for 5sec and second spread-out process conducts on 2000 RPM for 45 sec. Soft bake process pass off at 65 ℃ for 3 min and 95 ℃ for 9 min. The baked wafer is exposed on 400 mJ/cm^2. After exposure, the wafer is baked at 65 ℃ for 1 min and 95 ℃ for 7 min for develop, and the baked wafer is immersed in developer (SU-8 developer) for 8 min. the final step is hard bake which step reduces the residual stress and crack. In addition, this step firms the master mold.

To cast the mold, PDMS is cured on master mold. PDMS consist of elastomer (Sylgard 184, silicone elastomer base) and cure (Sylgard 184 silicone elastomer curing agent); the mixing rate is the 10-volume of elastomer with 1-volume of cure. The mixed PDMS is poured over the master mold and cured it in the oven for

2hr at 80 ℃. After curing, the PDMS is peeled off from master mold (Figure 2.2 (c)). Figure 2.3(c) is the master mold fabricated by photoresist and Figure 2.3 (d) is micro fluidic channel casted by PDMS.

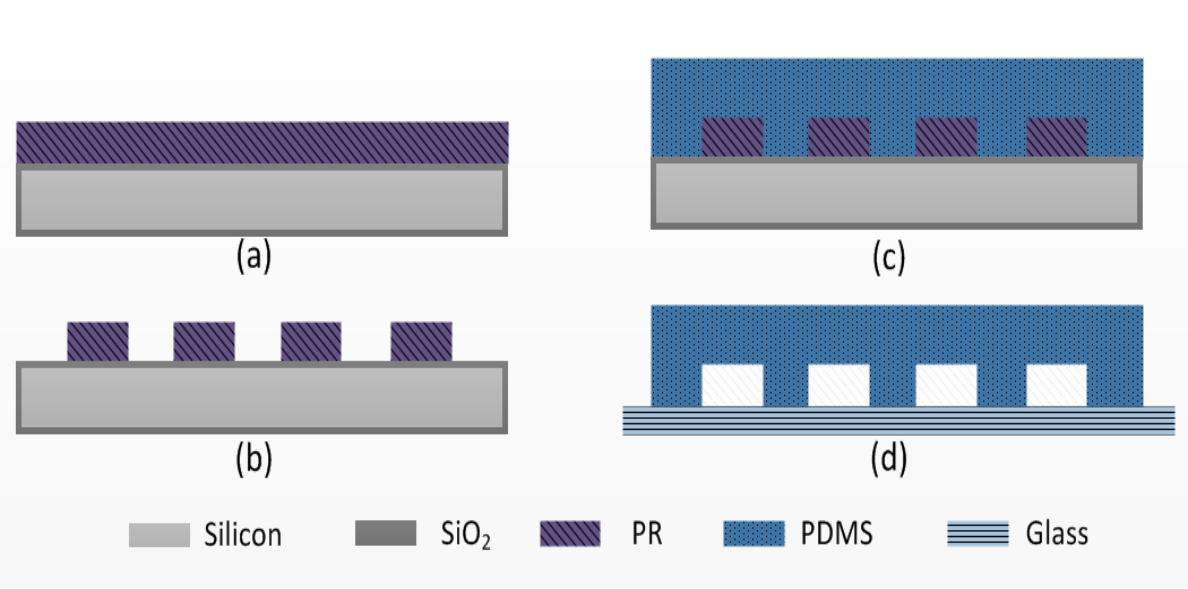

Figure 2.2 The flow chart to fabricate master mold for micro channel and PDMS channel; the spin-coating photoresist on substrate, (b) the exposure process for master mold, (c) casting the channel using PDMS, and (d) Bonding PDMS with slide glass.

2.2.3 Assemble the micro rotor and micro fluidic channel

This section explains the assembling process of the rotor and PDMS micro channel made form precedence process. The PDMS micro channel was drilled for tubing at the inlets and outlet using the punch (Harris Uni-Core 1.50). After that, the rotor is placed on PDMS channel and aligning the rotor with mixing chamber through the microscopy.

To bond PDMS channel to the slide glass, the surfaces of both contact side treat with oxygen plasma treatment. The plasma machine is FEMTO science CUTE-1MP/R. The recipe to bond them (Figure 2.2 (d)) is following; oxygen 60 sccm, power 100 W, and time 1 min. When finishing the oxygen treatment, PDMS channel and substrate, which treated surface, take out from plasma chamber, and PDMS channel fastens on substrate (Figure 2.4).

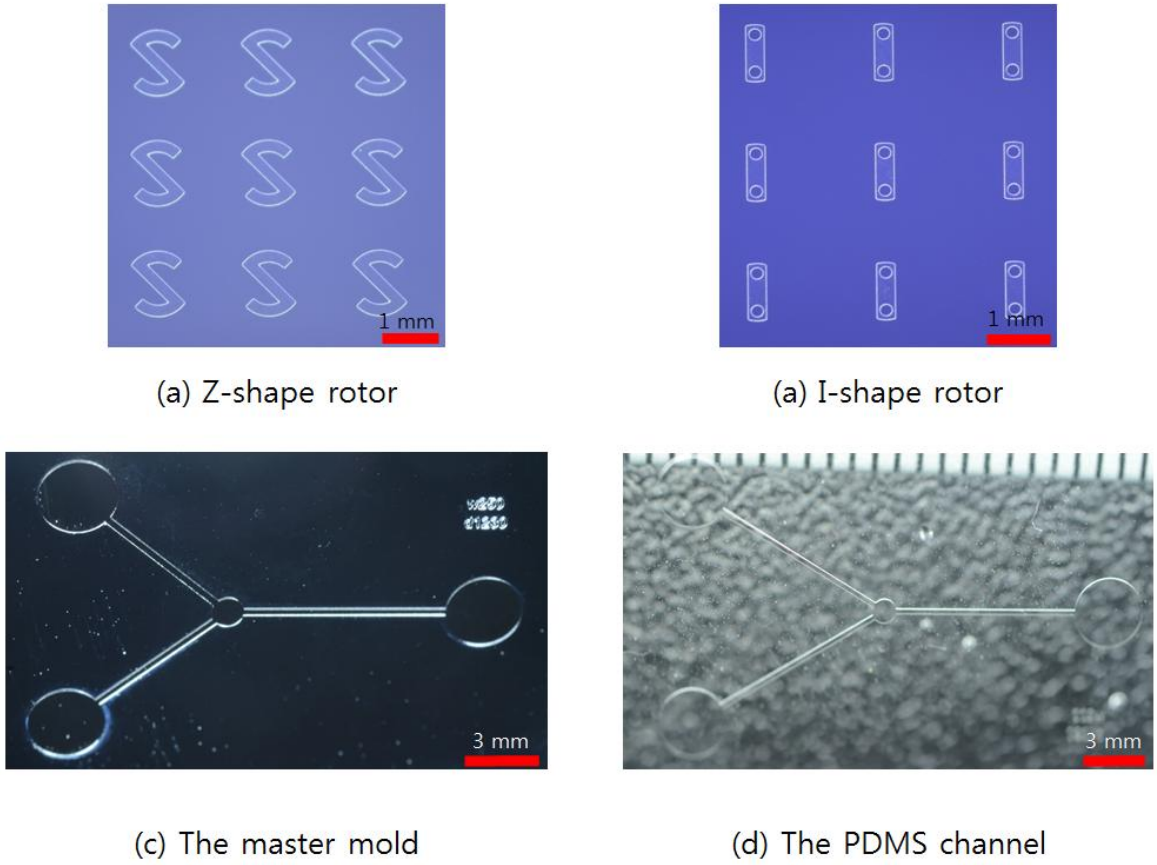

Figure 2.3 The components of micromixers; (a), (b) The fabricated rotors, (c) the master mold for micro fluidic channel, and (d) the PDMS channel.

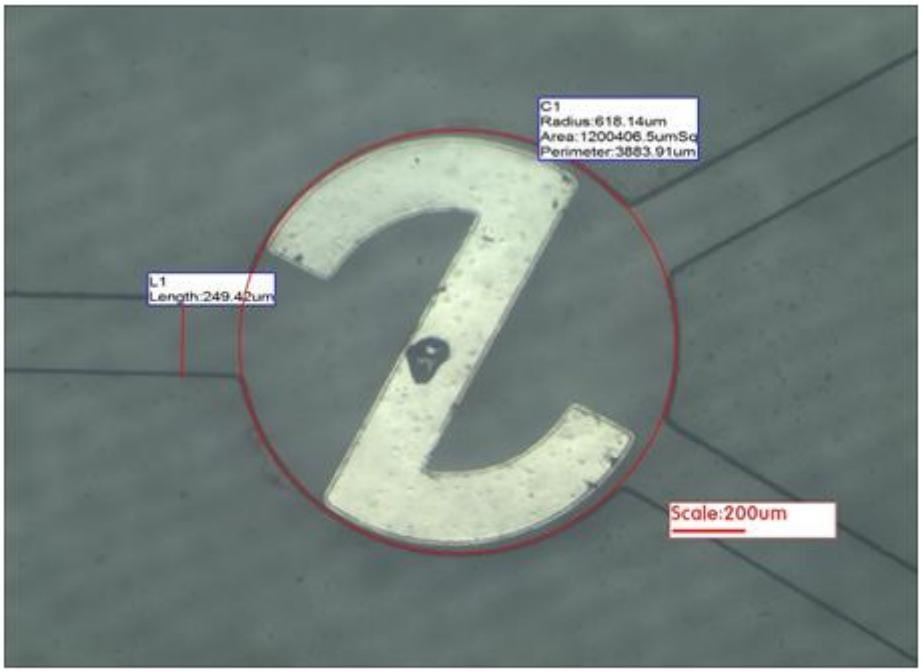

(a)

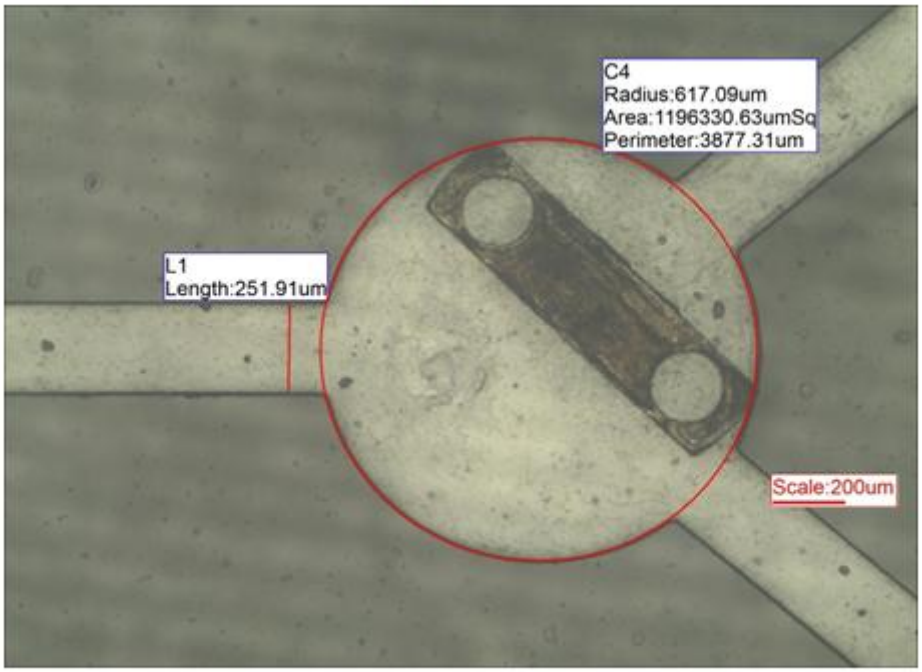

(b)

Figure 2.4 The whole image of assembled the mixing chamber and the magnetic rotor, (a) Z-shaped rotor and (b) I-shaped rotor.

3. EXPERIMENT AND ANALYSIS

3.1 Experimental setup

The suggested micromixer rotates following the spinning magnetic field. Thus, we have to set up the rotating magnetic field. There are two methods making the rotating field: rotating electromagnet and rotating permanent magnet attracted on motor. When making a rotating electromagnet, the system is more complex than rotating permanent magnet attracted on motor because the system of electromagnet should have a four electromagnetic coil to rotate the micromixer at on every side at least. However, another system based on motor is simple and able to control of rotation speed and rotating direction easily than electromagnetic system. Therefore, we set up the rotating permanent magnet based on motor. The rotation speed is controlled by adjusting the applying voltage and current to motor. The applying voltages are 6 and 8 V into motor. Figure 3.1 is the schematic diagram of rotating magnetic system. Figure 3.2 shows the real system to measure the mixing performance and take images of mixing process.

Evaluation of mixing performance was implemented by an image process method based on the assessment of the color intensity of mixture of dyed fluids. To analyze the mixed flow image, images were taken by high speed camera (Photron SA-3) during 10-sec with 500 frame-per-sec. the high camera should need to the bright light source so adding the three LED light source (Helieon 4100K, Molex 180081-4330). The light source focuses on the mixing chamber and channel.

The two different color fluids are red color ink and blue color ink for improving the color intensity when processing the image analysis. Red color ink is Winsor & newton Calligraphy ink (Scarlet), and blue color ink is Holbein drawing ink (cobalt blue). In addition, the experimental setup has the two syringe pumps. The one of pumps serves as the injection pump (KD scientific, KDS 210P) at inlets and another pump (Kent Scientifics, Genie plus) withdraws the mixed fluids at outlet. The conditions of flow rate are 500, 400, 300, 200, 100, 50, 25, and 10. The unit of flow rate is μL/hr.

Table 3.1 instructs the used device model name to experimental setup and Table 3.2 indicates the conversion information of the flow rate. The flow rate is volume rate so it cannot understand intuitionally to velocity or Reynolds number. Thus, we added the table to help understanding.

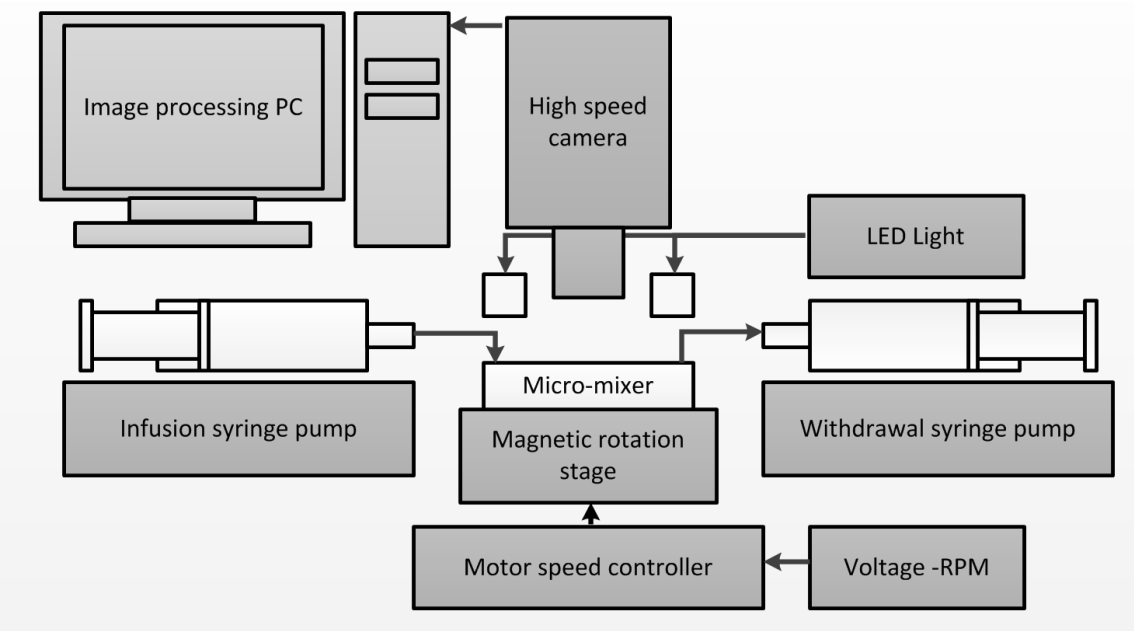

Figure 3.1 Schematic represents the experimental setup.

High speed camera	Photron SA-3
Lens	Edmund optics VZM 600i
Infusion Syringe pump	KD scientific KDS 210P
Withdraw syringe pump	Kent scientific Genie Plus
LED light	Helieon 4100K , Molex 180081-4330
Fan motor	Yate loon D80SM-72

Table 3.1 The equipment list used for the experiment.

Flow rate (μL/ hr)	Velocity (mm/s)	Reynolds number (dimensionless)
500	9.260	0.0640
400	7.407	0.0512
300	5.556	0.0384
200	3.704	0.0256
100	1.852	0.0128
50	0.926	0.0064
25	0.463	0.0032
10	0.185	0.0013

Table 3.2 The conversion table; the table shows that velocity and Reynolds number are converted from the flow rates.

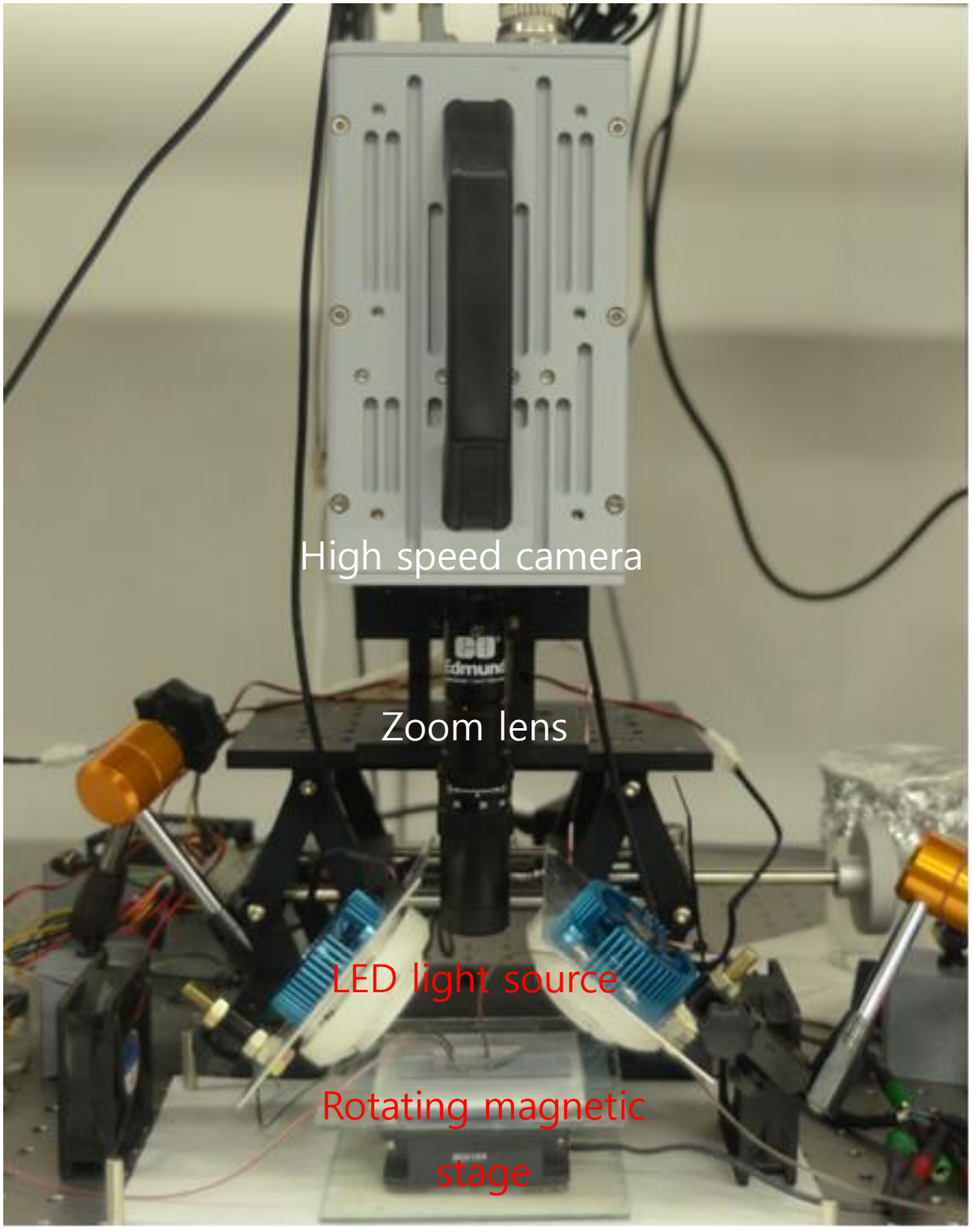

Figure 3.2 The whole picture of the experiment system; the rotating magnetic field and recoding system.

3.2 Image analysis to evaluate the mixing performance

Two methods are commonly used to evaluate the mixing performance: the dyed fluidic analysis method and the chemical reaction analysis method. The dyed fluidic analysis method can be split into two-methods which are the fluorescence dyeing method and the color dyeing method. The chemical reactions analyze divides into three methods: the pH indicator method and the competing method [16, 30, 31].

The mixture of blended fluid with not blended fluid can be observed in the fluorescence dyeing method. The mixing process image was taken by the CCD camera of the micro scope which has a filter only passing the permitted wave length. After, it measures the fluorescence intensity of each pixel of the Region of Interest (ROI) from the acquired image. Finally, it estimates the mixing performance using the mixed degree of fluorescence.

The color dyeing method is similar to the fluorescence dyeing method. First, the color dyed fluid was mixed with the not dyed fluid. After this, an image of the mixing process was taken by the CCD camera. This method can be verified by the naked eye because the difference of color light and shade is large. In addition, it is able to digitize an image using an image process measuring the intensity of each pixel in the ROI. During the mixing process, there is no reaction between the dyeing fluid and pure water in the channel so the color dyeing method is safe. Moreover, it shows the degree of mixing by diffusion or convection between the fluids [16].

The pH indicator method is the most popular method to evaluate mixing performance. The indicator has each color equivalent to pH. Based on the property of the indicator, it is able to quantify the mixing performance. The phenolphthalein indicator has a red color when mixing with fluid which has above eight pH. After mixing the phenolphthalein indicator with the sodium hydroxide, which has 13 pH, the mixed fluid color will change

from colorless to red following the pathway. This method is also checked by the fluidic color intensity by image process to measure the mixing performance. The methyl orange indicator and bromothymol blue solution (BTB solution) are able to serve as pH indicators instead of phenolphthalein. The methyl orange indicator has a red color, orange color, and yellow color when mixing with acid, neutral, and alkaline. The BTB solution, which is green at natural state, can also change from the original color to yellow and blue when reacting to acid and alkaline. Using the property of solutions, mixing performance was estimated through the image process.

The pH indicator method figures out the mixing index more easily than other methods, and is able to confirm the mixing process visually. However, the reaction time of the indicator and acid or alkaline is longer than the residual mixing time of the fluid in the mixing chamber, so the mixed fluid falls out of the mixing chamber without reacting. During that time, we could not apply this method.

The competing reaction method is using the chemical reaction. The chemical reaction formula is Equation (3.1). The competing reaction means that the reaction in the form of two or more proceeds in parallel concurrently [32].

$$\begin{aligned} &H^+ + Ac^- \rightarrow HAc \cdots\cdots\cdots\cdots\cdots\cdots (Ultrafast\ reaction) \\ &5I^- + IO_3^- + 6H^+ \rightarrow 3I_2 + 3H_2O \cdots\cdots\cdots\cdots (Fast\ reaction) \\ &I_2 + I^- \rightarrow I_3^- \cdots\cdots\cdots\cdots\cdots\cdots\cdots (Absorbing\ UV) \end{aligned} \quad \textbf{(3.1)}$$

The fast reaction is usually faster than other chemical reactions, but is slower than the ultrafast reaction relatively. Therefore, the ultrafast reaction occurs earlier than the fast reaction during the mixing process, at a

subsequent time, the fast reaction occurs steadily. When two fluids initially contact, even if the reaction is non-uniform, the ultrafast reaction happened first. After, a hydrogen ion (H^+) increases locally; it causes the fast reaction actively. In other words, when being made from a uniform mixture, an ultrafast is caused. However, it mostly generates a fast reaction when made up of a non-uniform mixture. At this time, the generated iodide ion (I_3^-) has the property of absorbing the ultraviolet light (UV). Using the nature of the iodide ion, the UV absorption factor was measured by a UV meter, and the mixing performance was evaluated by the UV absorption factor. This method is able to appraise mixing performance and is similar to phenomena of real chemical reactions. However, when increasing the gap between the mixing time and the measuring time, the portion of iodide ion is growing; therefore, the result of the measurement is less accurate. Thus, the UV absorption factor of the mixed fluids excreted from the mixing chamber has to be evaluated by using a UV meter.

As aforementioned, the methods for mixing performance are various evaluation means, but a good evaluation method should fulfill several conditions:

- Simple mixing schemes in order to avoid complex analysis of many products
- Easy analysis method of mixing products
- Good sensitivity and reproducibility

The color dyeing method satisfies the conditions. The color dyeing method shows the mixing performance utilizing the image process directly and visualizes the mixing process. The image of mixing process was taken by the high speed camera to analysis the mixing performance. The acquired images, which are the RGB (red,

green, blue) system, were converted to gray scale to present each pixel information by the eight-bit. The distribution of pixel intensity, which was expressed by eight-bit, means that mixing uniformity how much representing the mixed evenly. The Equation (3.2) expresses the mixing performance [33]. Using the gray scale amplitudes, a criterion index C_{dev} normalized by

$$C_{dev} = \frac{\sqrt{\frac{1}{N_p}\sum_{i=1}^{N_p}(I_i - I_{mean})^2}}{2^n - 1} \qquad \textbf{(3.2)}$$

Where N_p is the total number of the pixel, and I_i is the deviation of the pixel intensity. I_{mean} is the averaged intensity, and it serves as the reference of mixing uniformity in order to more effectively describe the mixture uniformity. *n* is the gray scale bit number of the image under analysis. In this paper, n is eight-bit. We applied red plane to enhance the red color. Thus, the intensity of each pixel was expressed from 0 for red to 255 for black.

The Equation (3.3) is suggested to objectify the evaluation index and compare between the different mixers performances. The Equation (3.2) considers not only the outlet of mixer but also the inlet of mixer. The improved mixing performance defined by

$$C_{mix} = \frac{C_{dev\_inlet} - C_{dev\_outlet}}{C_{dev\_inlet}} \qquad \textbf{(3.3)}$$

Where, C_{dev_inlet}, C_{dev_outlet} are C_{dev} of each inlet and outlet. If the mixer works completely, the I_i in Equation (3.2) is all the same. Thus, C_{mix} is become to one. The other way, when mixer does not work, C_{mix} is become zero. C_{mix} defined by Equation (3.3) is called by mixing uniformity [33].

The acquired images were calculated by MATLAB (Math works). We developed code to evaluate mixing performances automatically. Figure 3.3 shows the original acquired RGB image. The Figure 3.3 (a) is the RGB image before the mixture and Figure 3.3 (b) shows the mixture process. The measurement point was marked on Figure 3.3. Figure 3.5 shows the original RGB scale image (Figure 3.5 (a)) and the converted gray scale image (Figure 3.5 (b)) at initial state. In addition, the grapy expresses the color index at measurement point (Figure 3.6). The acquired color index was used when evaluating the mixing performance by Equation (3.3). Figure 3.5 (c) and (d) shows final image of among the acquired images. The images are the part of taken whole image (Figure 3.6(a), (b)). The mixing performance is zero before the mixing (Figure 3.6(c)) and the graph shows the color index each pixels. During the mixing, the mixing performance at measurement point (Figure 3.6 (d)) is 0.98 by Equation (3.3). It means that mixing performance is 98 percent. The graph represents that the distribution of color intensity is evenly. The more the difference between the pixels intensity is little, the more the mixing performance is better.

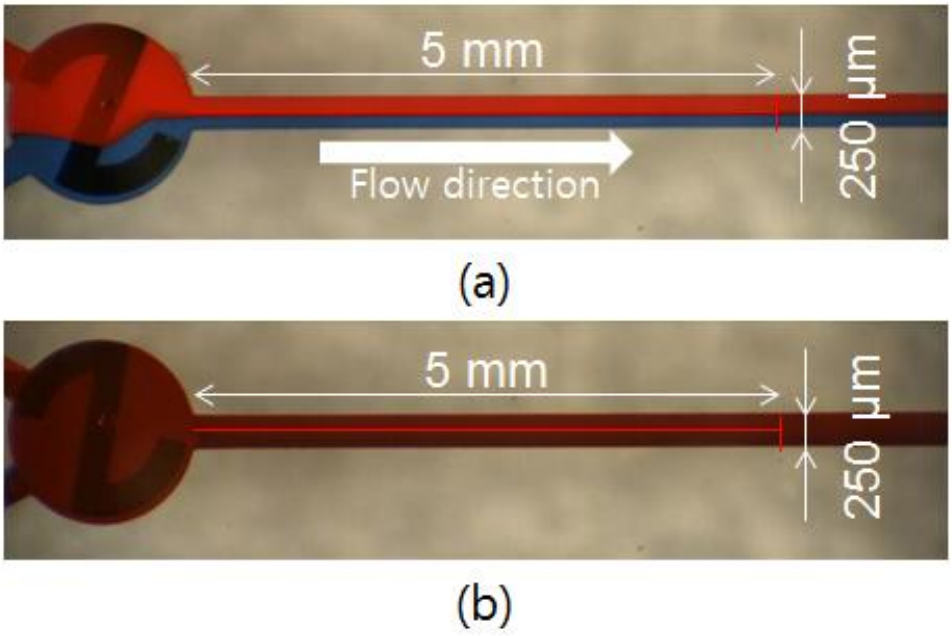

Figure 3.3 The measurement position for mixing performance more than 100 μL/ hr; (a) the image before mixing and (b) the image after mixing.

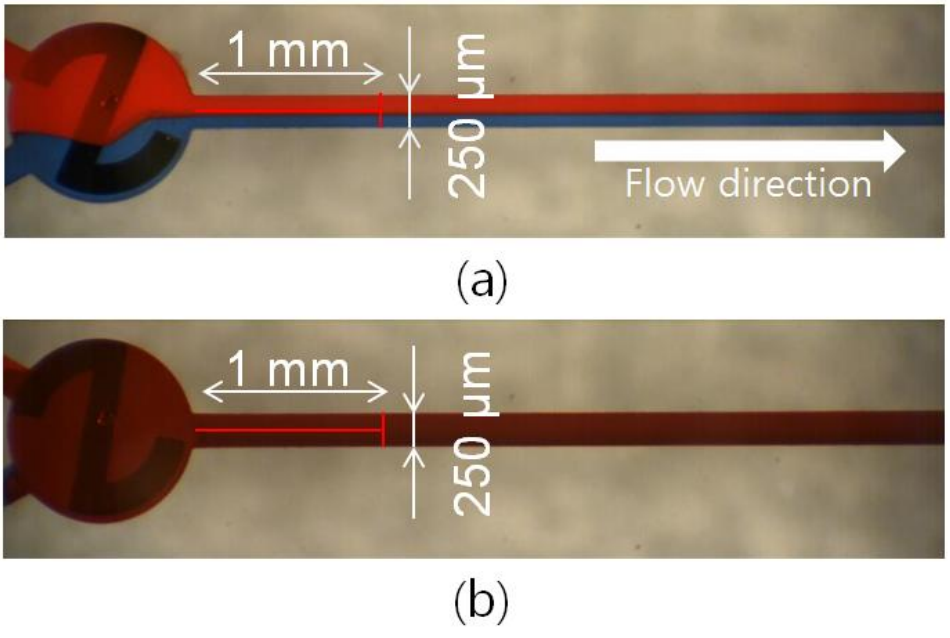

Figure 3.4 The measurement position for mixing performance under 100 μL/ hr; (a) the image before mixing and (b) the image after mixing.

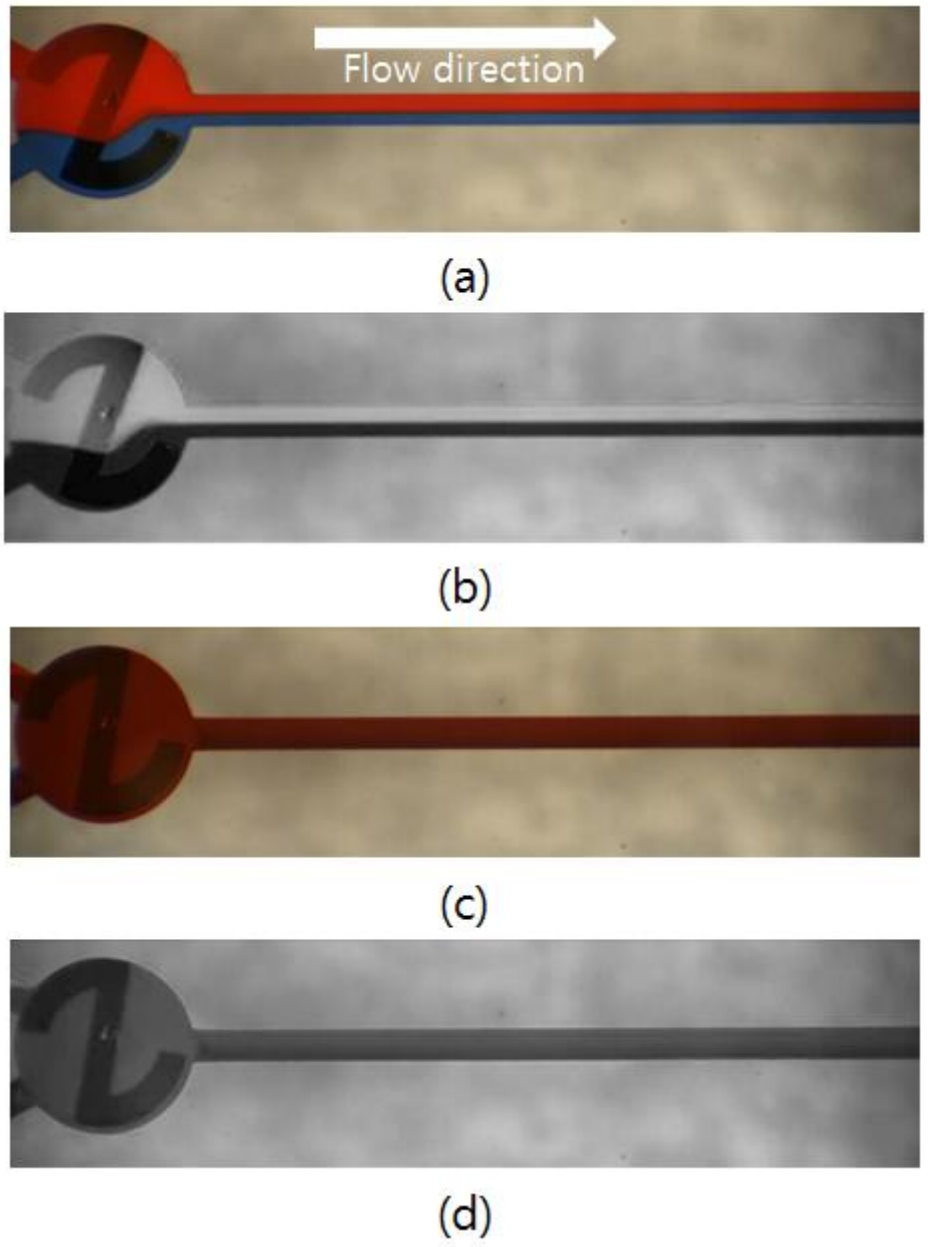

Figure 3.5 The original RGB images (a), (c) and images (b), (d) converted to gray scale; (a), (b) the images before mixing and (c), (d) the images after mixing.

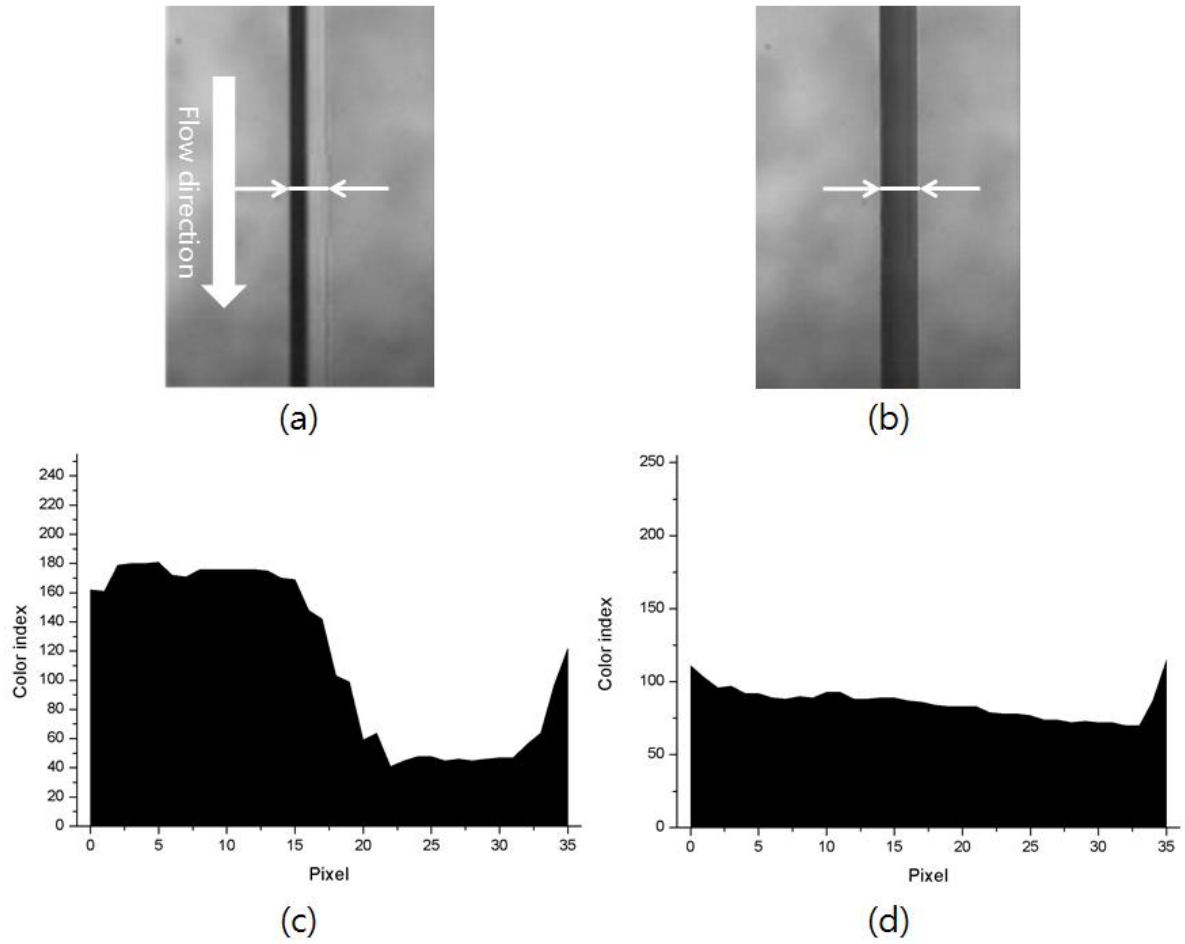

Figure 3.6 The measurement position and color index of pixels; (a) the part of the channel images before mixing, (b) the part of the channel images after mixing and (c), (d) the color index of measurement position.

4. RESULTS AND DISCUSSIONS

4.1 Experimental results

Figure 2.4 shows the fabricated micromixer in a 1230-μm-diameter and 60-μm-deep mixing chamber and flowing the two different color inks in a 250-μm-diameter and 60-μm-deep micro channel. The fabricated micromixer and micro channel carried out the mixing performance using the red color ink and blue color ink. Two different color inks mixed without the chemical reaction so we could observe the mixture with inks. Thus, this method is suitable to evaluate the objective mixing performance than the chemical reaction method. When the rotor operated to spin, it exerted momentum to the fluid, generating a confined ring-shaped motion of fluid particles.

The mixing performance was evaluated at distance of 5 mm from mixing chamber because of considered to measure the fully developed flow when flowing flow rate more than 100 μL/hr (Figure 3.3). If flow rate is under 100 μL/hr, the distance is 1 mm away from the mixing chamber (Figure 3.4). The reason of measuring the 1 mm away from exit of chamber is that the mixed fluids cannot reach a distance of 5 mm from exit of chamber during 10 sec. However, in these cases, the discharged flow from chamber is fully developed flow. Thus, length for developing to steady state is not necessary.

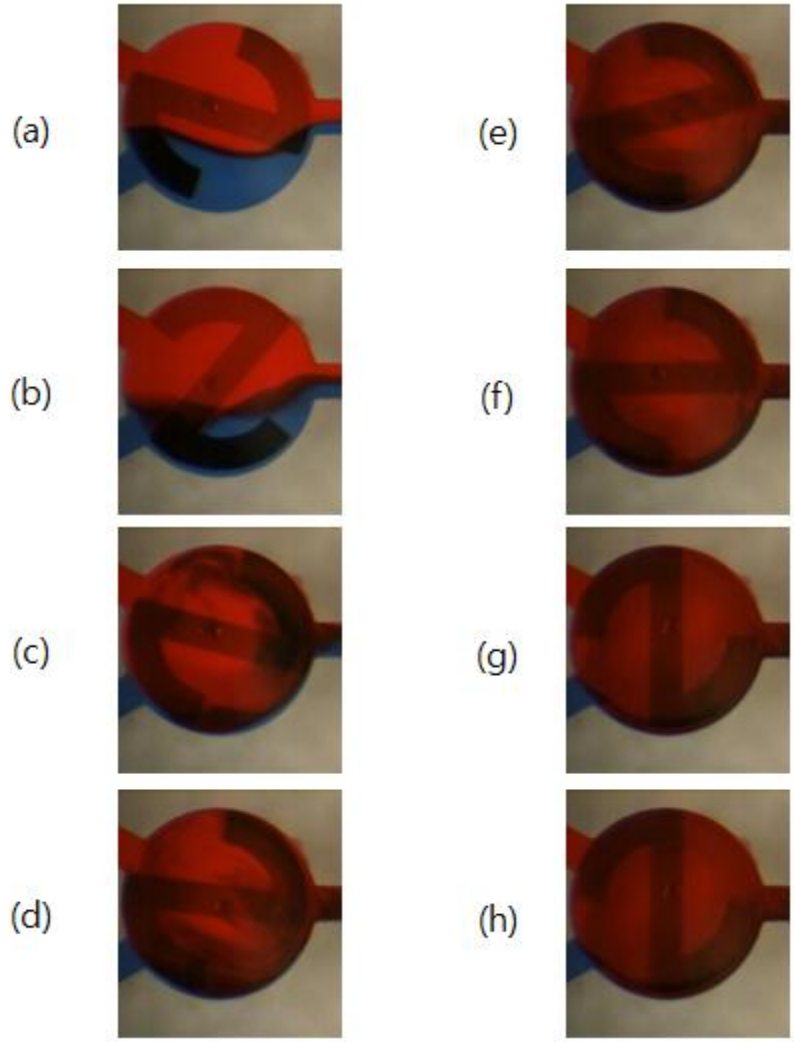

Figure 4.1 The observation of mixer motion as 0.5 sec.

The internal pressure interrupts the flow and motion of rotor so it has to be solved. The internal pressure occurs when assembling all things to test. Thus, the syringe pumps should be stabilized before the test. The internal pressure removal method is to disconnect the tube linked with channel with needle connected syringe pumps withdraw side until fluids do not flow out from tube assembling all things to test.

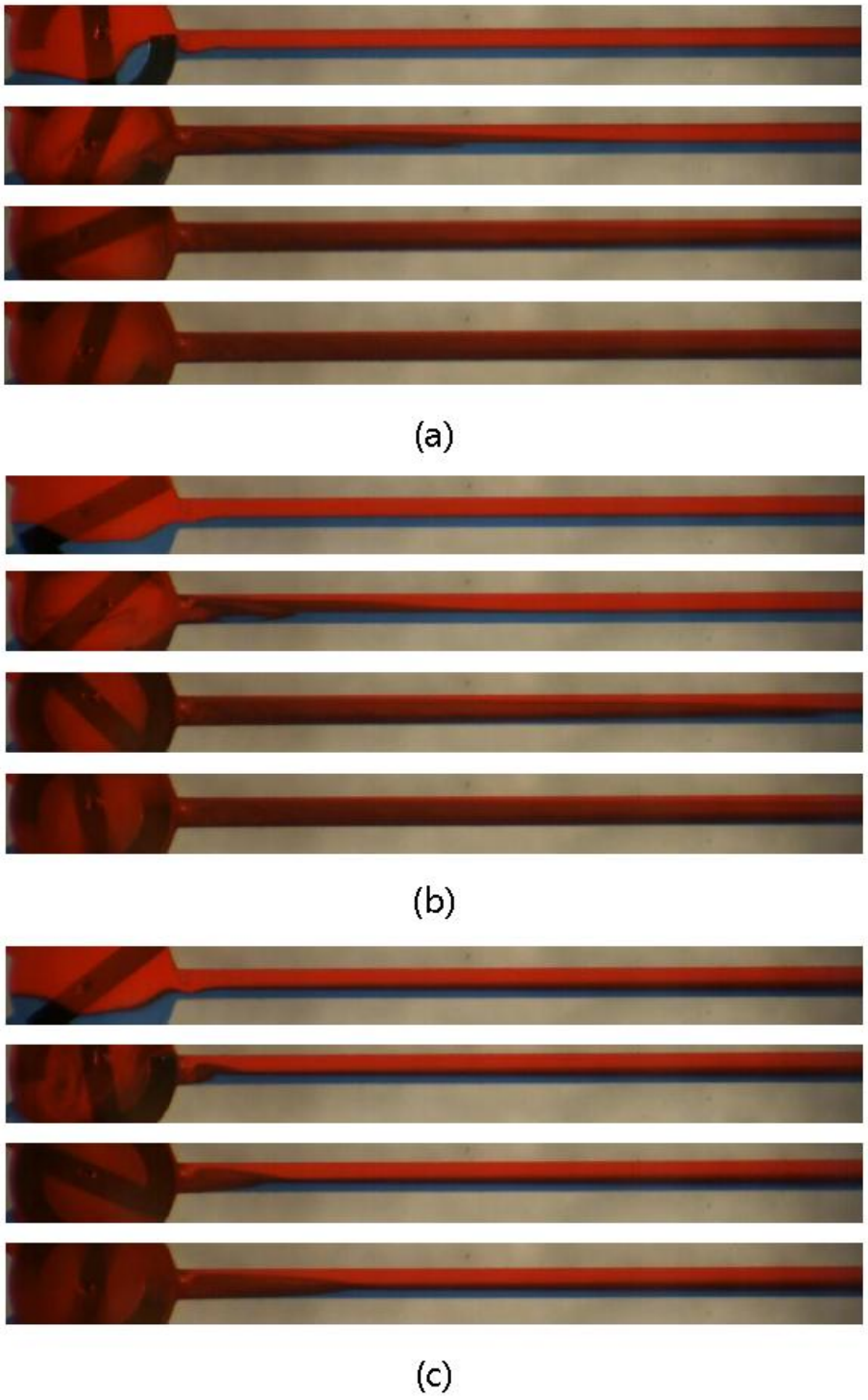

Figure 4.2 The distance comparison with different speed at 250 msec period; (a) the flow rate is 200 μL/hr, (b) the flow rate is 100 μL/hr , and (c) the flow rate is 50 μL/hr, applying 8 V, Z-shaped rotor.

Figure 4.3 shows the mixing performances of each 70 percent, 80 percent, 90 percent, and 95 percent. The mixing performances are expressed by the Equation (3.2) and Equation (3.3) which calculates the standard deviation of pixel.

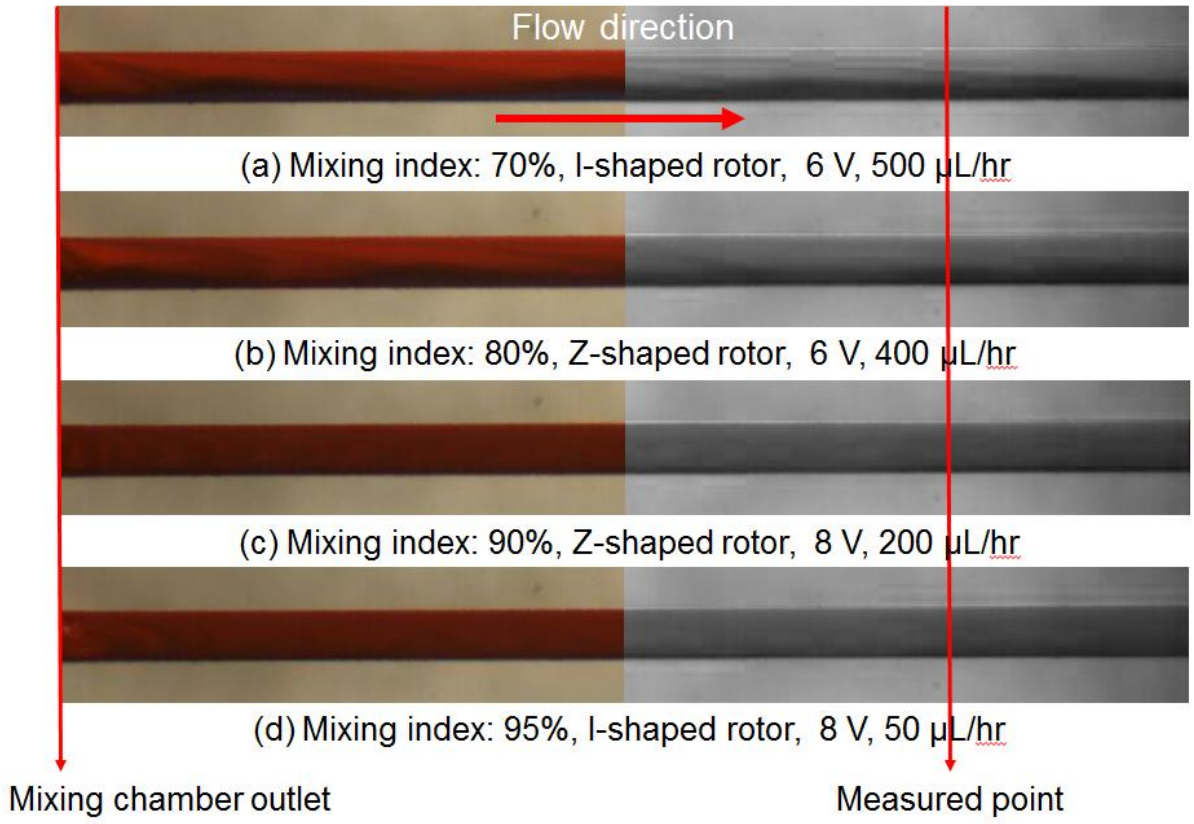

Figure 4.3 The mixing performance and conditions.

Figure 4.4 (a) and (b) have the transition section during from 2 sec to 5sec at 400 μL/hr, and 500 μL/hr flow rates. The reason having the transition section is that the section of 0 to 2 sec is the rotor acceleration area to spin following the rotating magnet, but the section is deceleration area due to the drag force of fluid.

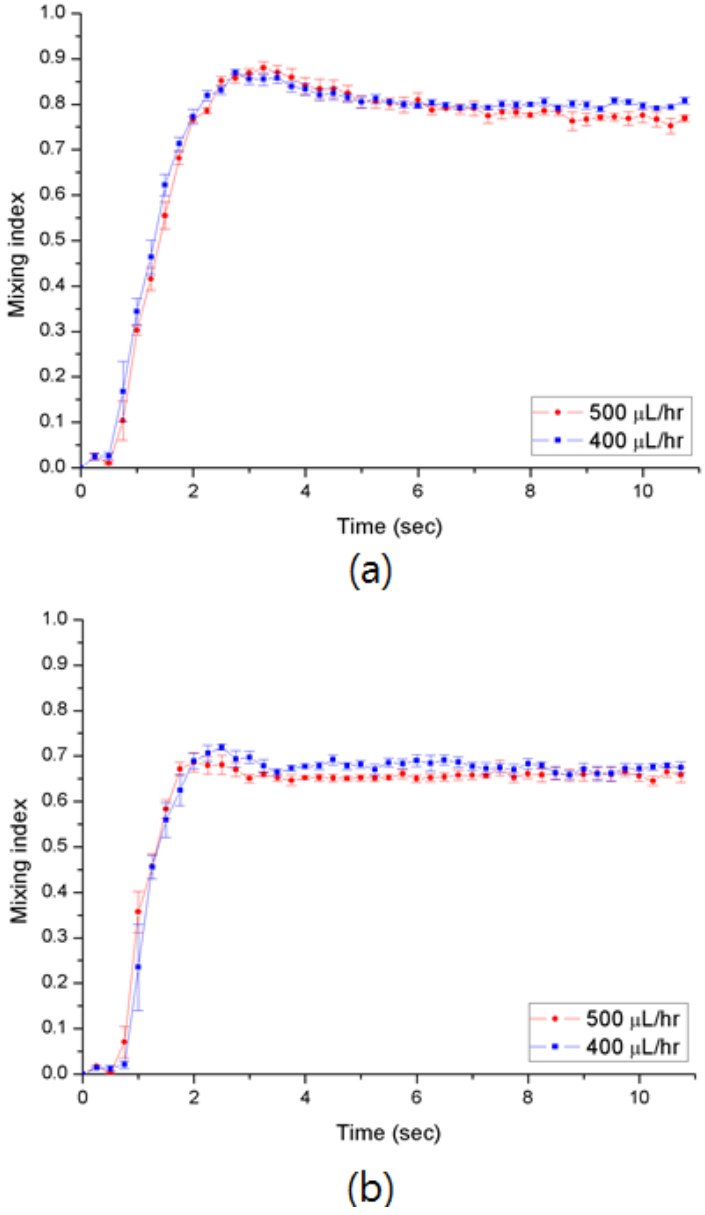

Figure 4.4 The results of different shape with applying 6 V into motor; (a) the Z-shaped rotor, (b) the I-shaped rotor.

Figure 4.5 (b) of rotating I-shaped rotor has also the transition section during from 2 sec to 4sec, when applied 8V. From the flow rate 400 μL/hr, it has a low standard deviation. It means that the distribution of pixel intensity is narrow at ROI. However, the flow rate 500 μL/hr line shows a high standard deviation.

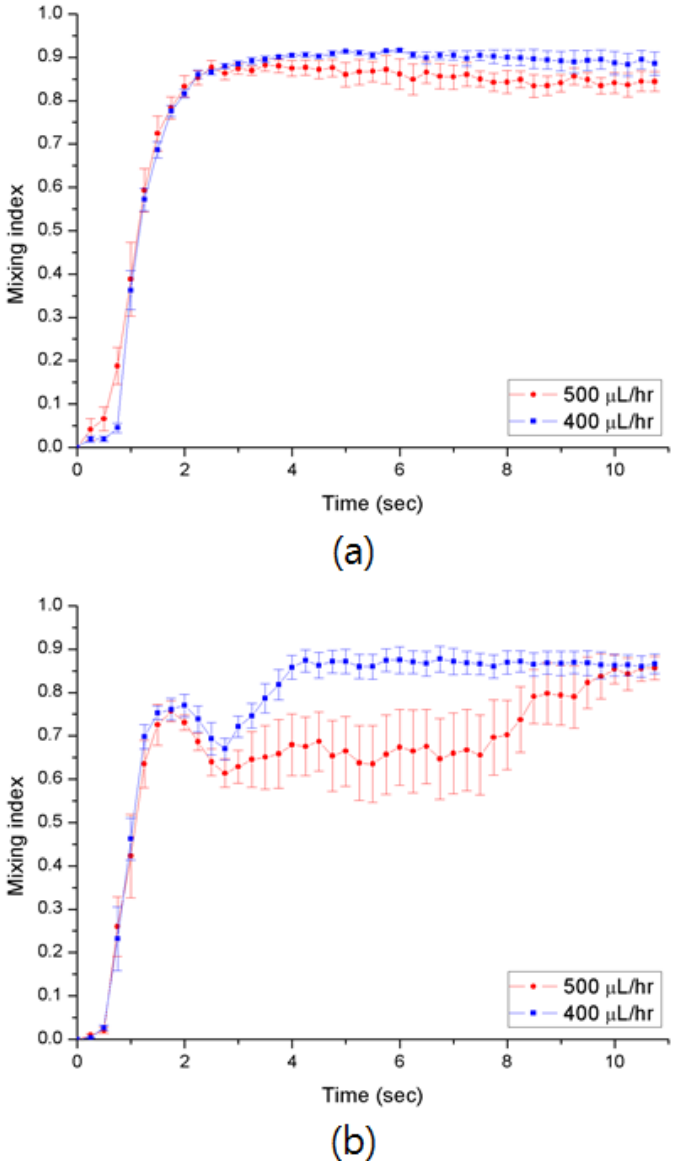

Figure 4.5 The results of different shape with applying 8 V into motor; (a) the Z-shaped rotor, (b) the I-shaped rotor.

In other words, the distribution of pixel intensity distributed widely at ROI. Those results were achieved by experiments every five times at same conditions. In five times test, the micromixer might be stuck in mixing chamber due to the friction between with PDMS wall at least one times. The drag force by fast flow rate generates the friction and impedes the rotating motion of stir.

When operating the same conditions with the Z-shaped rotor, the rotor shows good motion than I-shaped rotor because the shape and inertia of the each rotor are different. When spinning Z- shaped rotor, the wings of stir-bar help the rotating motion from friction and guide the orbit. In addition, the wings of rotor keep the momentum to rotate stir. Thus, Z-shaped rotor shows better performance than I-shaped rotor at same conditions.

Figure 4.6 was drawn the mixing performances with following the conditions; the conditions are the same shape and the different applying voltage. To see the Figure 4.6, the graphs explain the better mixing performance than when decreasing the flow rate. The Z-shaped rotor shows the linear lines at section from 100 to500, and the I-shaped rotor draws the linear lines at section from 200 to500. The Z-shaped rotor Figure 4.6 (a) distributes the results around 95% under flow rate 100 at different applying voltage. However, the I-shaped rotor Figure 4.6 (b) draws the line from 90 % to 97 % growing the performance with decreasing the flow rate and different applying voltage. The I-shaped rotor shows a tendency that the rotation speed is marginal factor at low flow rate such under flow rate 50.

The points are results of mixing performance when applying the same voltage and the different shape. Figure 4.7 (a) is the results with same applying 6-voltage to motor, the results are that Z-shaped rotor is better 10 % than I-shaped rotor performance at from 500 to 100 section. However, the gap of performance is not much at fewer than 100 sections. Figure 4.7 (b) is the results with same applying 8-voltage to motor, the results are similar all section. This graph said that the area gap of rotor is able to overcome by the rotation speed.

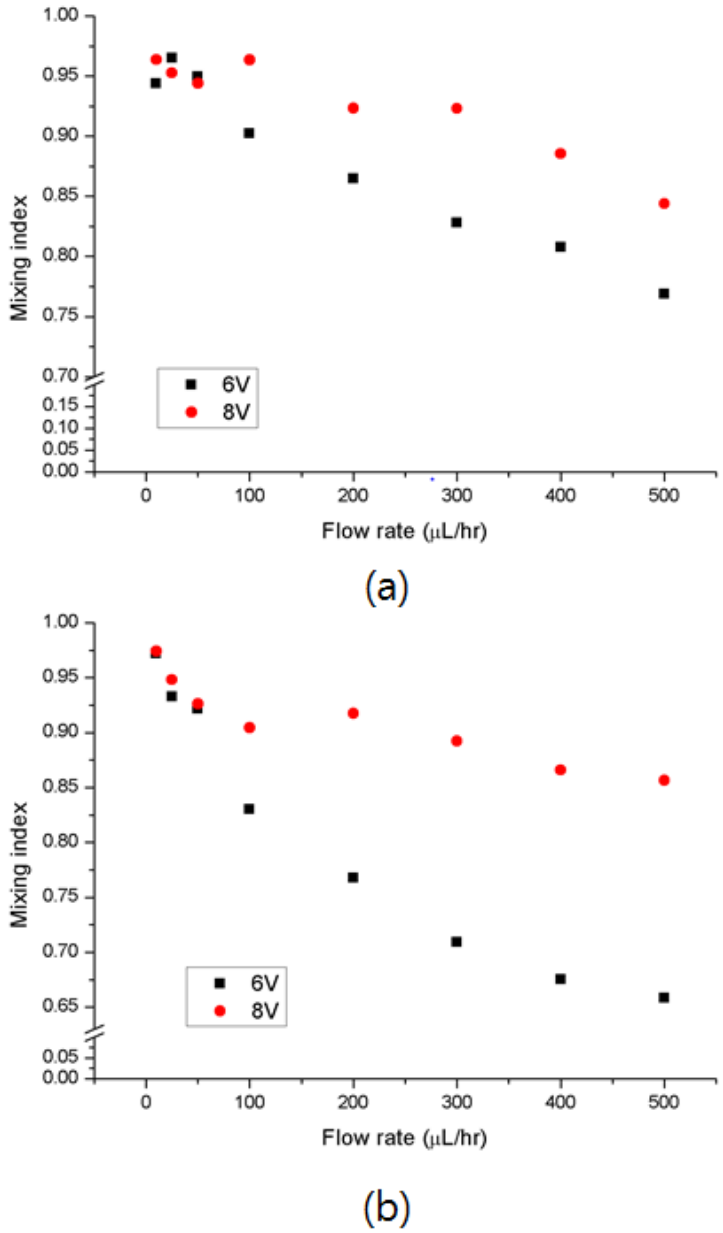

Figure 4.6 The mixing performances as same shape with different applying voltage; (a) the Z-shaped rotor and (I) the I-shaped rotor.

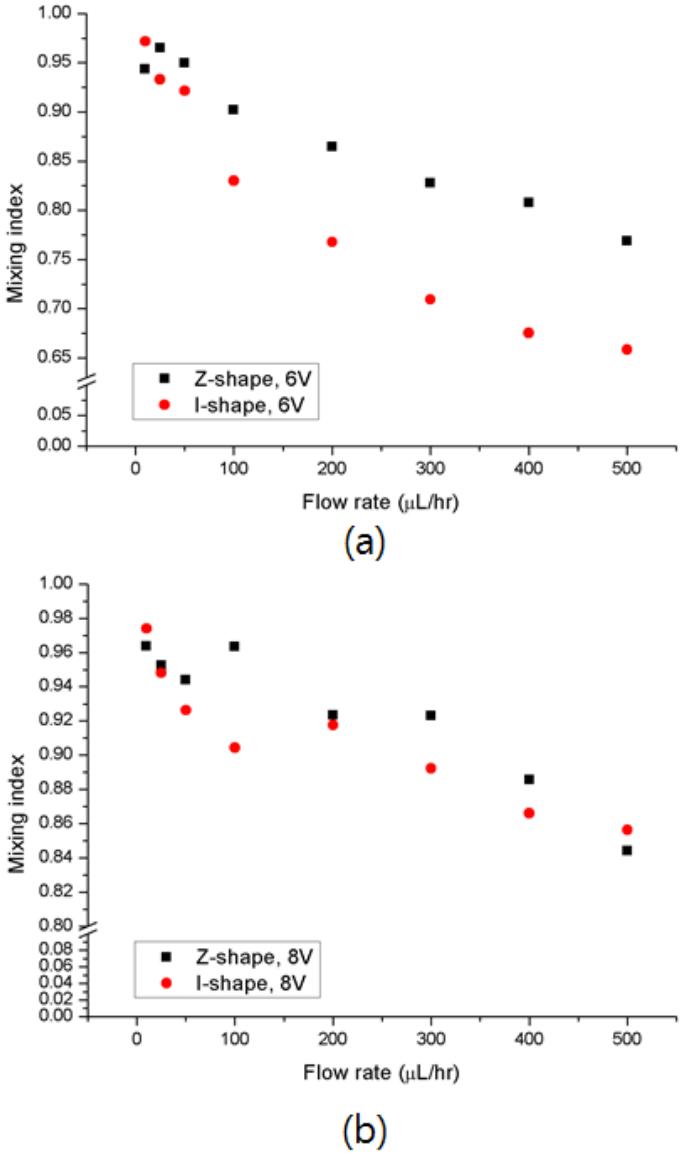

Figure 4.7 The mixing performance as applying same voltage and different shapes; (a) the mixing performance of different shapes with the applying 6 V into motor and (b) the mixing performance of different shapes with the applying 8 V into motor.

Figure 4.8 expressed the performances following a Reynolds number from 0.001 to 0.1. The mixing performance is better than a high Reynolds number. It means the flow rate dominates at same Reynolds number which is same characteristic length, cross section area and viscosity of inks. Which the flow rate is slow represents that the residual time is long than fast flow rate and the contact area increases between fluids.

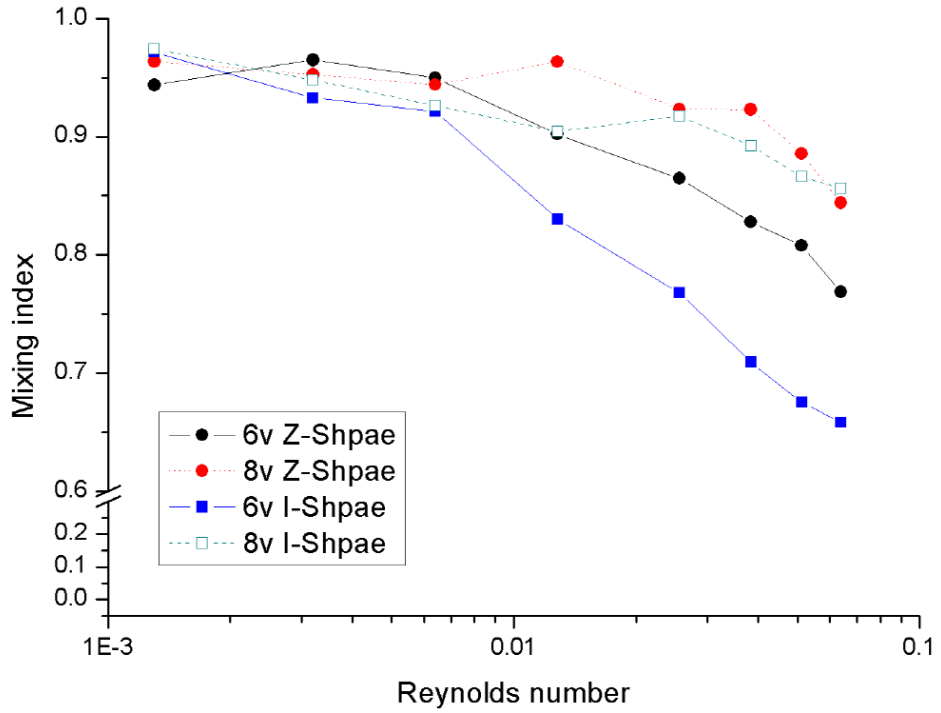

Figure 4.8 The results of mixing as Reynolds numbers.

4.2 Discussions

This thesis used the two different color inks to observe the mixing performance. However, the other researchers commonly used the DI water and methyl blue alcohol or methyl blue alcohol and methyl orange alcohol for mixing. If it uses the deionized water (DI water) and methyl blue alcohol to monitor the mixing

performance, it shows better results than previous experiments. Its viscosities are different of inks versus DI water and methyl blue alcohol.

The present experimental setup assembled the rotating magnetic field module and the stage for mixing so the stage is vibrating with rotation module when the applying voltage increases to grow motor rotation speed. The stage is vibrating so we could not get the results over the 8 voltage. However, when separating the stage and rotation module, we can get the better results than the present setup and the fabricated chip is free from vibration effect. This thesis used the applying voltage instead of the rotation speed but if adding the RPM date, it supports the results objectively, and helps understanding to readers.

The rotor is 2-dimensional structure but changing the structure to 3-dimensional improves the performance. Besides, the I-shaped rotor is stuck in chamber some times. It needs to change the design. When adding the wing at each end, wings help the rotation, and prevents stuck. In addition, we assume that it saving the momentum to spin. Finally, the Lab chips are used in biological field. To use the fabricated rotor in biological field, the fabrication process has to add the additional process which the coat process to biocompatible materials such gold and titanium.

5. CONCLUSIONS

The micromixers are essential to mixing in micro fluidic chips flowing low Reynolds number fluids. The mixture defends on diffusion in fluids being a low Reynolds number. To generate diffusion, the chips have a narrow width and a long length channel to short a diffusion length. However, the chips have size limitation, so it is not enough to locate the long and narrow channel. Researchers have studied making short diffusion length by changing the channel structure or generating the chaotic advection.

This thesis designed the active type mixer which gets external energy to mix fluids to expect using field required a high mixing performance. The fabricated active mixer rotates by torque which is generated by rotating magnetic field. The designed mixer was fabricated by electroplating with Nickel-Cobalt alloy and the micro channel was made by PDMS to flow fluids. The fabricated micro channel is simple Y-shape to observe only the mixing performance.

The rotating magnetic field was made by motor and permanent magnet, and the rotating magnetic stir performance was evaluated by image process objectively. That time, the mixing performance was confirmed with various flow rates which are 10, 25, 50, 100, 200, 300, 400, and 500 L/hr, and applying voltages are 6 V and 8 V.

The results said that the slower flow rates shown the better performances than the fast flow rates. Because the mixing performance is mainly depend on the residual time in mixing chamber and channel. The fast flow has the short residual time and the slow flow has the long residual time. In other words, the long residual time give the more chance to contact between the fluids than the fast flow. In addition, when rotating low RPM

(applying 6-voltage), it showed the performance gap between different areas of rotor. The area of Z-shaped rotor is wider than I-shaped rotor. Thus, the performance difference from the gap of rotor area is around 10% at applying 6 V into motor. However, the performance difference is no little odds when applying 8-voltage. It means that the area difference has not an effect on mixing index at applying 8 V into motor.

This thesis confirmed the possibility of mixer of the fabricated micro magnetic rotor, and evaluated the mixing performance by analyzing the image. The fabricated micro magnetic mixer is fabricated on low cost and assembled easily.

REFERENCES

[1] C.-M. Ho and Y.-C. Tai, "Micro-electro-mechanical-systems (MEMS) and fluid flows," *Annual Review of Fluid Mechanics,* vol. 30, pp. 579-612, 1998.

[2] J. W. Judy, "Microelectromechanical systems (MEMS): fabrication, design and applications," *Smart materials and Structures,* vol. 10, p. 1115, 2001.

[3] A. D. Stroock, S. K. Dertinger, A. Ajdari, I. Mezić, H. A. Stone, and G. M. Whitesides, "Chaotic mixer for microchannels," *Science,* vol. 295, pp. 647-651, 2002.

[4] C. D. Chin, V. Linder, and S. K. Sia, "Lab-on-a-chip devices for global health: past studies and future opportunities," *Lab on a Chip,* vol. 7, pp. 41-57, 2007.

[5] L. H. Augenlicht and D. Kobrin, "Cloning and screening of sequences expressed in a mouse colon tumor," *Cancer research,* vol. 42, pp. 1088-1093, 1982.

[6] R. Daw and J. Finkelstein, "Lab on a chip," *Nature,* vol. 442, pp. 367-367, 2006.

[7] P.-A. Auroux, D. Iossifidis, D. R. Reyes, and A. Manz, "Micro total analysis systems. 2. Analytical standard operations and applications," *Analytical Chemistry,* vol. 74, pp. 2637-2652, 2002.

[8] D. R. Reyes, D. Iossifidis, P.-A. Auroux, and A. Manz, "Micro total analysis systems. 1. Introduction, theory, and technology," *Analytical chemistry,* vol. 74, pp. 2623-2636, 2002.

[9] R. S. Pawell, D. W. Inglis, T. J. Barber, and R. A. Taylor, "Manufacturing and wetting low-cost microfluidic cell separation devices," *Biomicrofluidics,* vol. 7, p. 056501, 2013.

[10] P. S. Dittrich, K. Tachikawa, and A. Manz, "Micro total analysis systems. Latest advancements and trends," *Analytical Chemistry,* vol. 78, pp. 3887-3908, 2006.

[11] K. F. Jensen, "Microreaction engineering—is small better?," *Chemical Engineering Science,* vol. 56, pp. 293-303, 2001.

[12] J. J. Abbott, K. E. Peyer, M. C. Lagomarsino, L. Zhang, L. Dong, I. K. Kaliakatsos, *et al.*, "How should microrobots swim?," *The international journal of Robotics Research,* vol. 28, pp. 1434-1447, 2009.

[13] H. Song, J. D. Tice, and R. F. Ismagilov, "A microfluidic system for controlling reaction networks in time," *Angewandte Chemie,* vol. 115, pp. 792-796, 2003.

[14] N. Rott, "Note on the history of the Reynolds number," *Annual review of fluid mechanics,* vol. 22, pp. 1-12, 1990.

[15] J. Holman, "Heat Transfer. 2002," ed: McGraw Hill, NY.

[16] K. S. Ryu, K. Shaikh, E. Goluch, Z. Fan, and C. Liu, "Micro magnetic stir-bar mixer integrated with parylene microfluidic channels," *Lab on a Chip,* vol. 4, pp. 608-613, 2004.

[17] N.-T. Nguyen and Z. Wu, "Micromixers—a review," *Journal of Micromechanics and Microengineering,* vol. 15, p. R1, 2005.

[18] M. Kakuta, F. G. Bessoth, and A. Manz, "Microfabricated devices for fluid mixing and their application for chemical synthesis," *The Chemical Record,* vol. 1, pp. 395-405, 2001.

[19] V. Hessel, S. Hardt, H. Löwe, and F. Schönfeld, "Laminar mixing in different interdigital micromixers: I. Experimental characterization," *AIChE Journal,* vol. 49, pp. 566-577, 2003.

[20] N. Schwesinger, T. Frank, and H. Wurmus, "A modular microfluid system with an integrated micromixer," *Journal of Micromechanics and Microengineering,* vol. 6, p. 99, 1996.

[21] P. Gravesen, J. Branebjerg, and O. S. Jensen, "Microfluidics-a review," *Journal of Micromechanics and Microengineering,* vol. 3, p. 168, 1993.

[22] F. Schönfeld, V. Hessel, and C. Hofmann, "An optimised split-and-recombine micro-mixer with uniform 'chaotic'mixing," *Lab on a Chip,* vol. 4, pp. 65-69, 2004.

[23] I. Glasgow and N. Aubry, "Enhancement of microfluidic mixing using time pulsing," *Lab on a Chip,* vol. 3, pp. 114-120, 2003.

[24] X. Niu and Y.-K. Lee, "Efficient spatial-temporal chaotic mixing in microchannels," *Journal of Micromechanics and Microengineering,* vol. 13, p. 454, 2003.

[25] M. Oddy, J. Santiago, and J. Mikkelsen, "Electrokinetic instability micromixing," *Analytical Chemistry,* vol. 73, pp. 5822-5832, 2001.

[26] H. H. Bau, J. Zhong, and M. Yi, "A minute magneto hydro dynamic (MHD) mixer," *Sensors and Actuators B: Chemical,* vol. 79, pp. 207-215, 2001.

[27] L.-H. Lu, K. S. Ryu, and C. Liu, "A magnetic microstirrer and array for microfluidic mixing," *Microelectromechanical Systems, Journal of,* vol. 11, pp. 462-469, 2002.

[28] Y. Yamanishi, Y.-C. Lin, and F. Arai, "Magnetically modified PDMS microtools for micro particle manipulation," in *Intelligent Robots and Systems, 2007. IROS 2007. IEEE/RSJ International Conference on,* 2007, pp. 753-758.

[29] M. Riahi and E. Alizadeh, "Fabrication of a 3D active mixer based on deformable Fe-doped PDMS cones with magnetic actuation," *Journal of Micromechanics and Microengineering,* vol. 22, p. 115001, 2012.

[30] Z. Yang, S. Matsumoto, H. Goto, M. Matsumoto, and R. Maeda, "Ultrasonic micromixer for microfluidic systems," *Sensors and Actuators A: Physical,* vol. 93, pp. 266-272, 2001.

[31] V. Hessel, S. Hardt, H. Löwe, A. Müller, and G. Kolb, "Chemical Micro Process Engineering, vols. 1 and 2," ed: Wiley-VCH, Weinheim, 2005.

[32] M.-C. Fournier, L. Falk, and J. Villermaux, "A new parallel competing reaction system for assessing micromixing efficiency—experimental approach," *Chemical Engineering Science,* vol. 51, pp. 5053-5064, 1996.

[33] Y. Z. Liu, B. J. Kim, and H. J. Sung, "Two-fluid mixing in a microchannel," *International journal of heat and fluid flow,* vol. 25, pp. 986-995, 2004.

요 약 문

회전 자기장 기반의 능동형 마이크로 믹서의 제작과 성능 평가

레이놀즈 수 낮은 유체가 흐르는 마이크로 플루이딕 칩에서 서로 다른 유체를 혼합하기 위한 믹서는 필수적이다. 낮은 레이놀즈 수를 갖는 유체를 혼합하기 위해서는 확산에 의존해야 하는데, 확산이 잘 일어나는 조건은 채널의 폭이 좁고, 채널의 길이가 길어야 한다. 하지만 마이크로 플루이딕 칩은 크기의 제한이 있어 충분한 확산이 일어나기 위한 충분한 길이를 칩 내에 형상화하기에 어려움이 있다. 이를 극복하기 위해 채널을 3 차원 구조로 변화시켜 확산 거리를 짧게 만든다거나, 혼돈 이류를 만드는 연구가 활발히 진행되고 있다.

하지만 보다 뛰어난 혼합성능을 필요로 하는 분야에 사용될 것을 기대하며 외부로부터 얻은 에너지를 혼합하는데 사용하는 능동형 믹서를 설계하였다. 제작된 능동형 믹서는 회전 자기장에 의해 발생되는 토크를 기반으로 회전하는 원리를 이용하였다. 제작된 로터는 자성물질인 니켈 코발트로 전기 도금 공정을 거쳐 제작되었다. 그리고 유체가 흐를 수 있게 마이크로 채널을 PDMS 를 이용하여 제작하였다. 채널은 믹서의 성능만을 보기 위해 Y-자 모양의 간단한 구조로 설계하였다.

자성 물질 로터를 돌리기 위해 영구자성을 모터를 연결하여 회전자기장을 구현하였고, 선회하는 자기장을 따라 회전하는 로터의 성능을 이미지처리 기반으로 성능을 객관화 하였다. 유량에 변화를 주고 또한 모터에 전압을 6 볼트와 8 볼트를 인가하여 다양한 실험조건을 바탕으로 자기장 혼합기의 성능을 평가하였다. 0.01 이하의 레이놀즈 수를 갖는 유체를 혼합 할 때는 로터의 모양, 회전수에 관계없이 90 퍼센트 이상의 성능을 보았다. 하지만 0.01 이상의 레이놀즈 수를 갖는 유체의 경우 회전수가 낮은 경우에는 로터의 면적이 넓은 것이 약 10% 정도 우수한 성능을 보였고, 회전수가 높은 경우에는 로터의 면적에 관계없이 비슷한 성능을 내는 것을 확인하였다.

실험을 위해 제작된 회전 자기장 스테이지와 마이크로 혼합기를 올려두는 스테이지가 결합되어 있는 구조로 제작된 현재의 실험환경에서는 8 볼트를 초과하는 전압을 가하였을 때 스테이지의 떨림으로 실험 데이터를 얻을 수 없었다. 하지만 추후에 두 스테이지를 분리하여 제작한다면 더 높은 전압을 가할 수 있어 현재보다는 더 높은 유량에서도 충분한 혼합성능을 보여줄 것으로 기대된다. 그리고 니켈코발트 합금으로 구성된 로터를 생체 적합한 물질로 코팅을 하면 생화학 및 화학 물질을 분석하는데 바로 이용가능 할 것으로 보여진다.

핵심어: 마이크로 플루이딕, 자기장 혼합기, 미세 혼합기, 자기장 엑츄에이션, 이미지 해석